Post Glacial Rebound and Relative Sea Level

- ΔRSL = ΔOSL + ΔGIA+ ΔVCM

- ΔVCM
  - largest probable signals on 100-year timescale
  - areas of large ΔVCM
  - California ΔVCM = earthquake cycle + crustal fluids
  - Many coastal cities have large VCM

RSL - relative sea level
OSL - ocean sea level
GIA - glacial isostatic adjustment
VCM - vertical crustal motion

Spatial and temporal variations in continental ice sheets

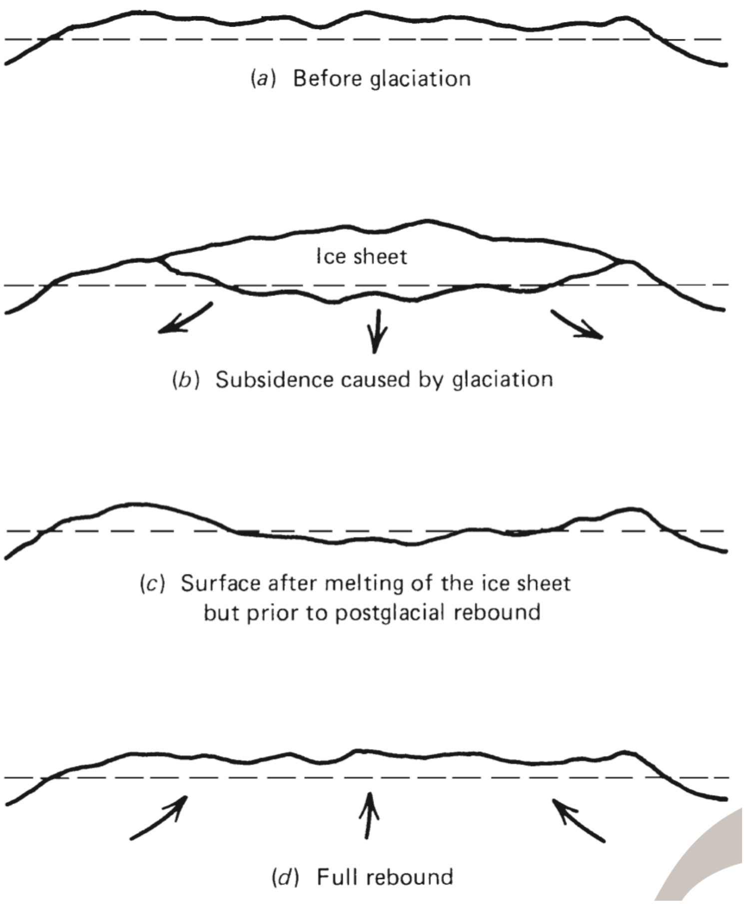

Figure 6.14 Subsidence due to glaciation and subsequent postglacial rebound
[Turcotte and Schubert, 2001]

J.L. Fastook, T.J. Hughes / Quaternary Science Reviews 80 (2013) 169–194

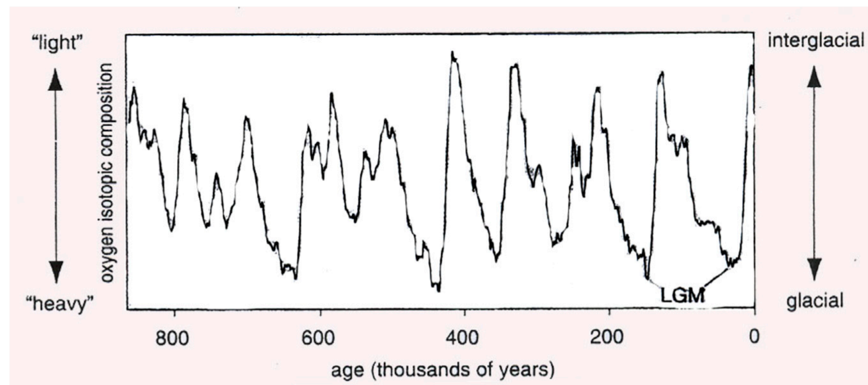

The progression of glaciation cycles through the Quaternary Ice Age using oxygen-isotope ratios as a proxy for global ice volume. LGM is the Last Glacial Maximum. From Siegert et al. (2002).

Major northern hemisphere continental ice sheets

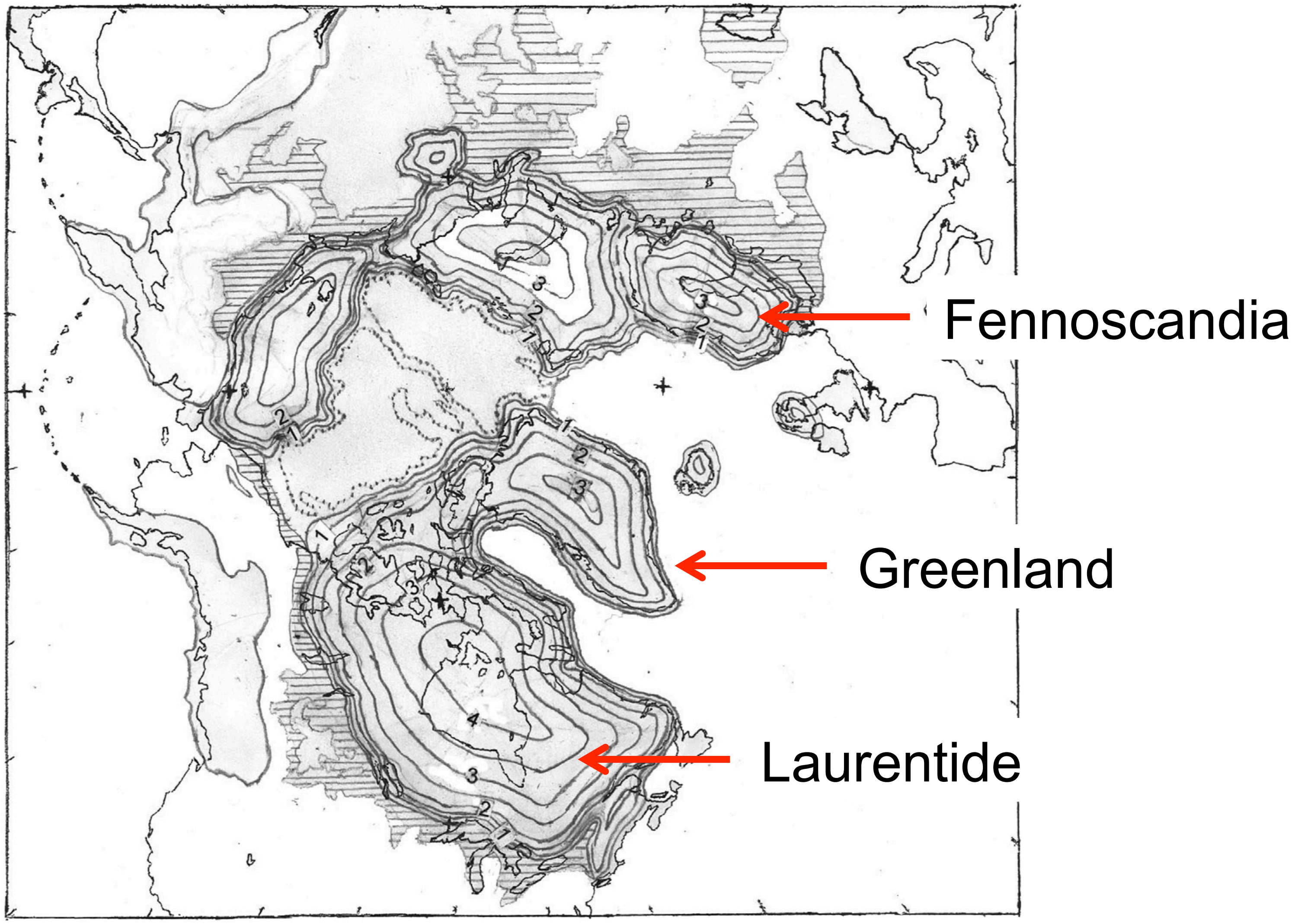

Fig. 6. Possible retreat configuration of Northern Hemisphere ice sheets during a Quaternary glaciation cycle obtained from bottom-up modeling. Ice shelves floating over basins in the Arctic Ocean are grounded along dotted lines. Ice-sheet elevations are contoured every 500 m, and labeled every kilometer. Ice sheets meet along broken suture lines. Mountain glaciations are enclosed by heavy lines. Proglacial lakes and other lakes are denoted by parallel horizontal lines.

Major northern hemisphere continental ice sheets

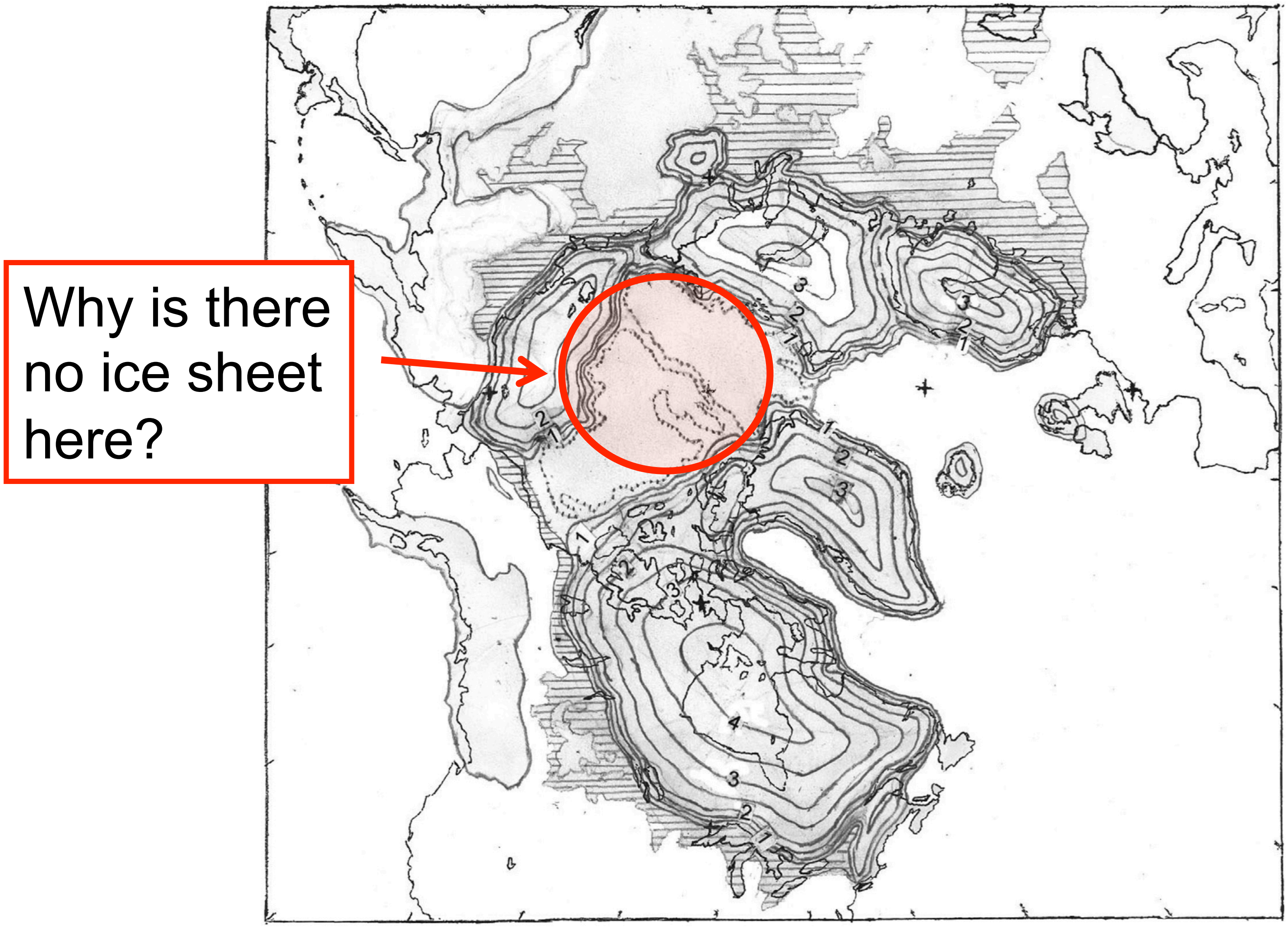

Fig. 6. Possible retreat configuration of Northern Hemisphere ice sheets during a Quaternary glaciation cycle obtained from bottom-up modeling. Ice shelves floating over basins in the Arctic Ocean are grounded along dotted lines. Ice-sheet elevations are contoured every 500 m, and labeled every kilometer. Ice sheets meet along broken suture lines. Mountain glaciations are enclosed by heavy lines. Proglacial lakes and other lakes are denoted by parallel horizontal lines.

Figure 1: Relative Sea Level

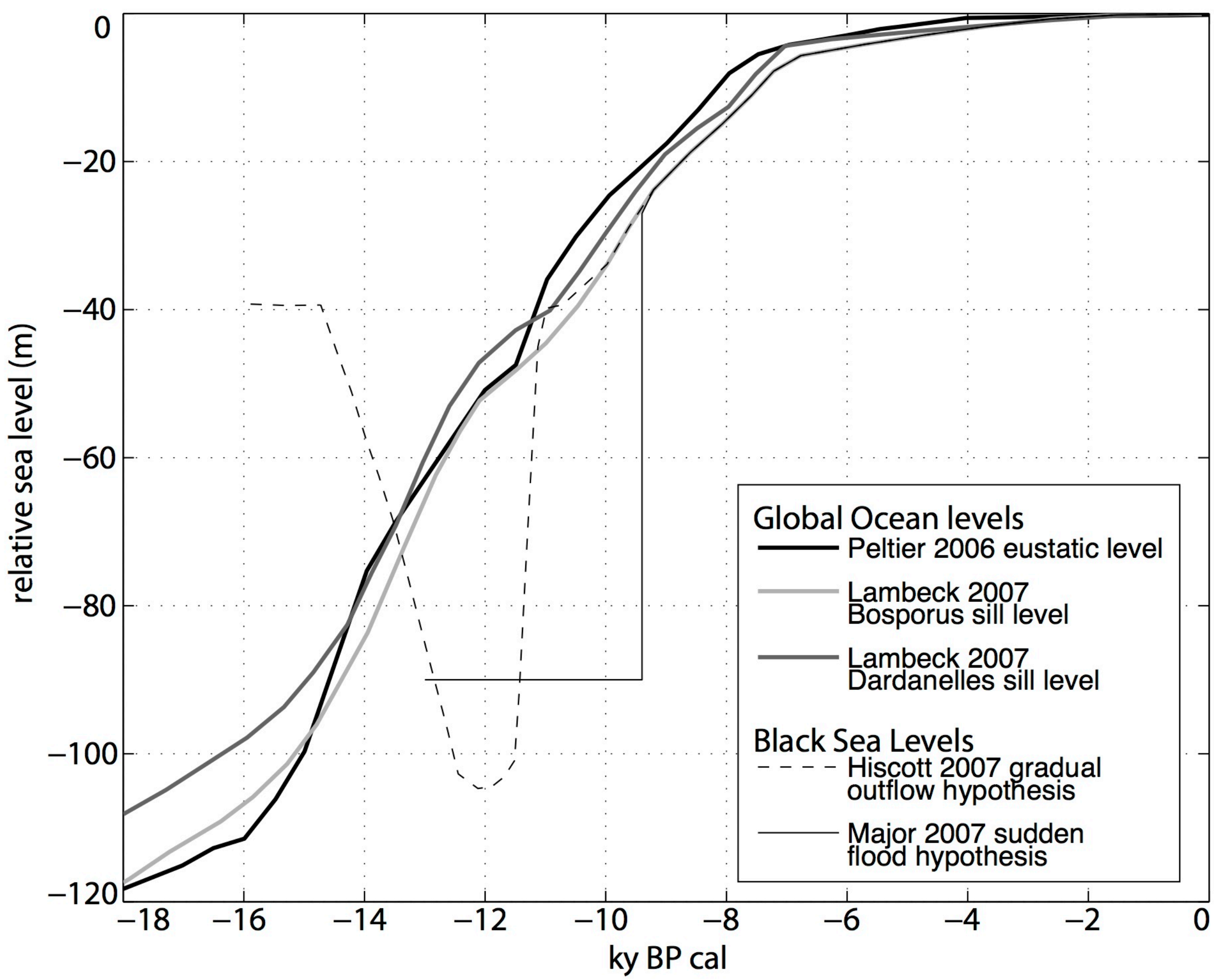

Uplift decreases exponentially with time

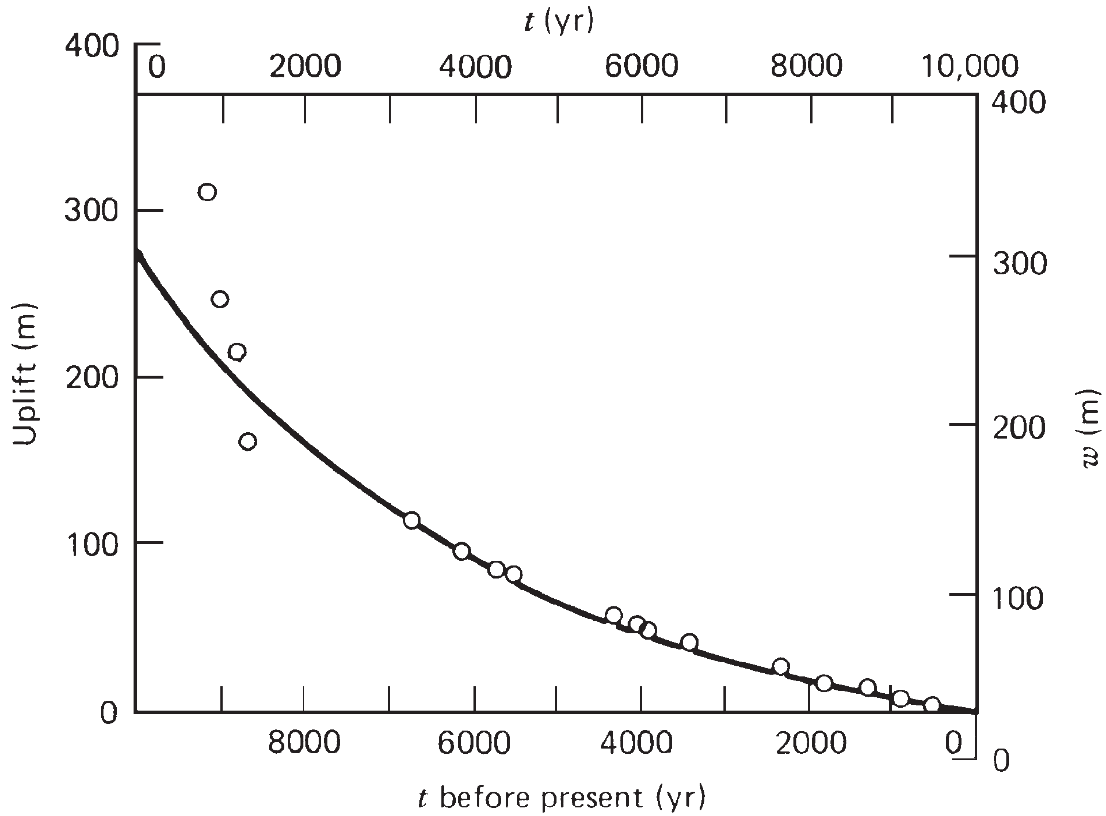

Figure 6.16 Uplift of the mouth of the Angerman River, Sweden, as a function of time before the present compared with the exponential relaxation model, Equation (6.104), for $w_{m_0} = 300$ m less 30 m of uplift yet to occur, $\tau_r = 4400$ years, and an initiation of the uplift 10,000 years ago.

Uplift Rate from GPS

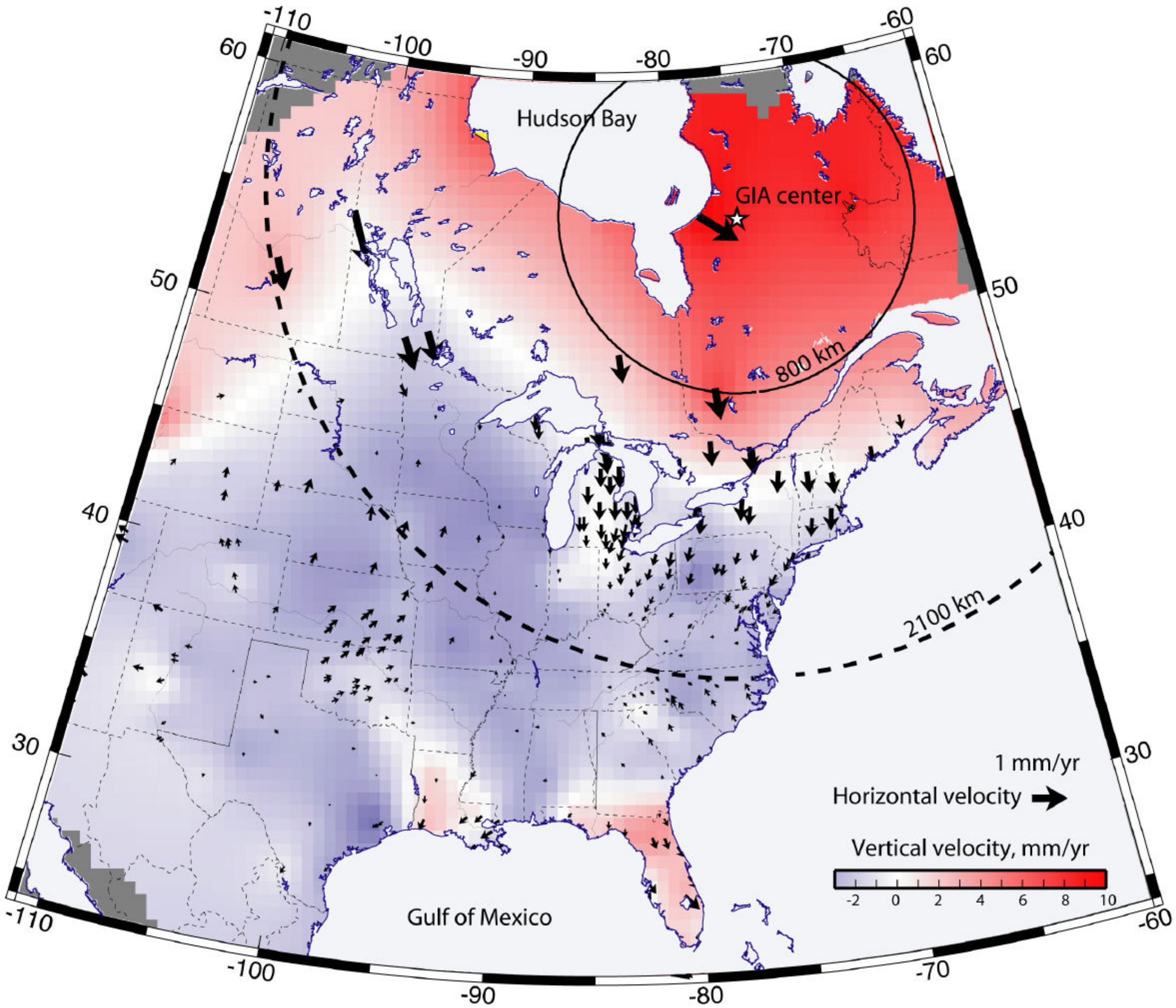

http://web.ics.purdue.edu/~ecalais/projects/noam/noam/

Laurentide rebound centered at Hudsons Bay

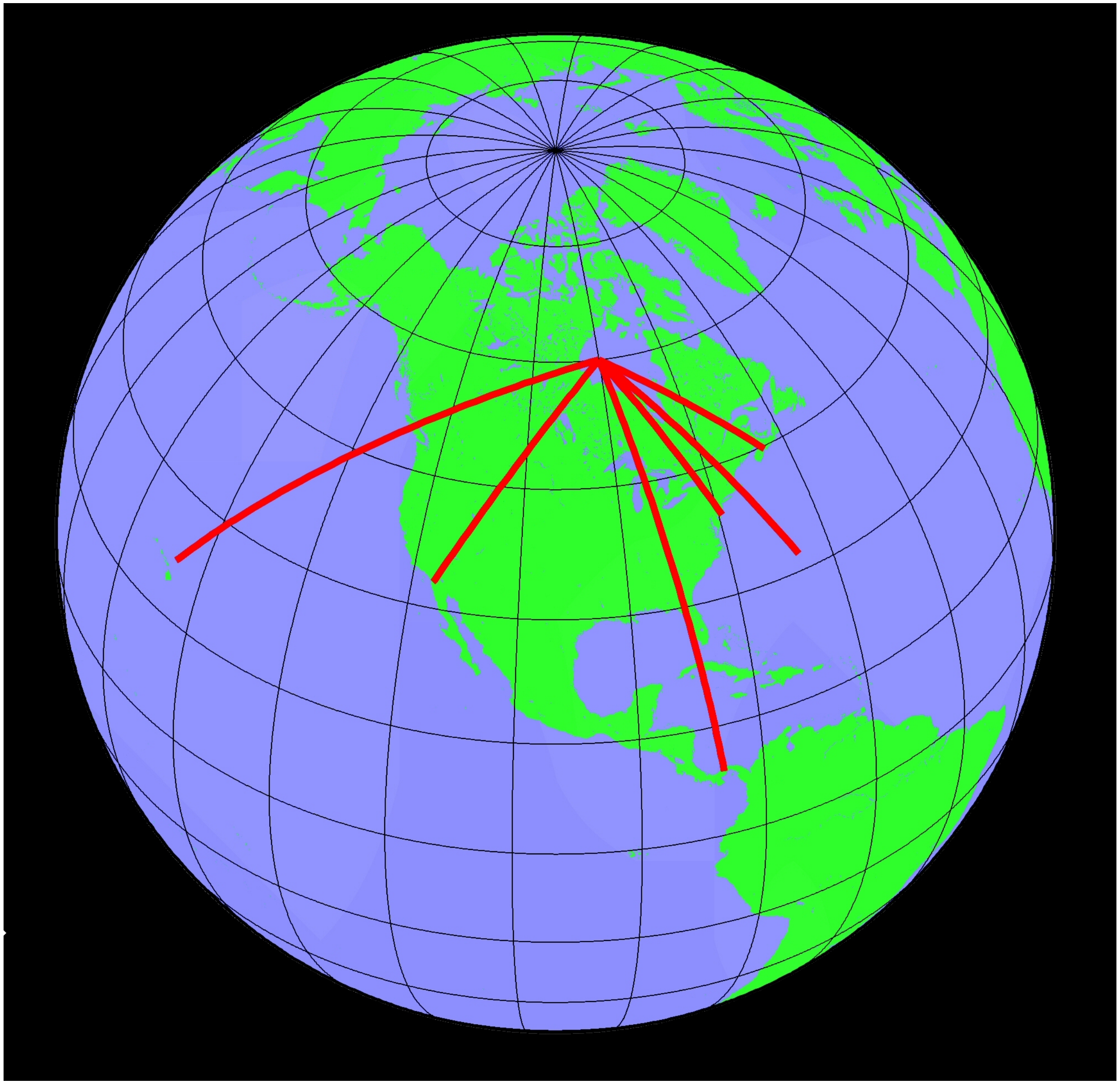

Miller L , and Douglas B C Phil. Trans. R. Soc. A 2006;364:805-820

RSL from tide gauges

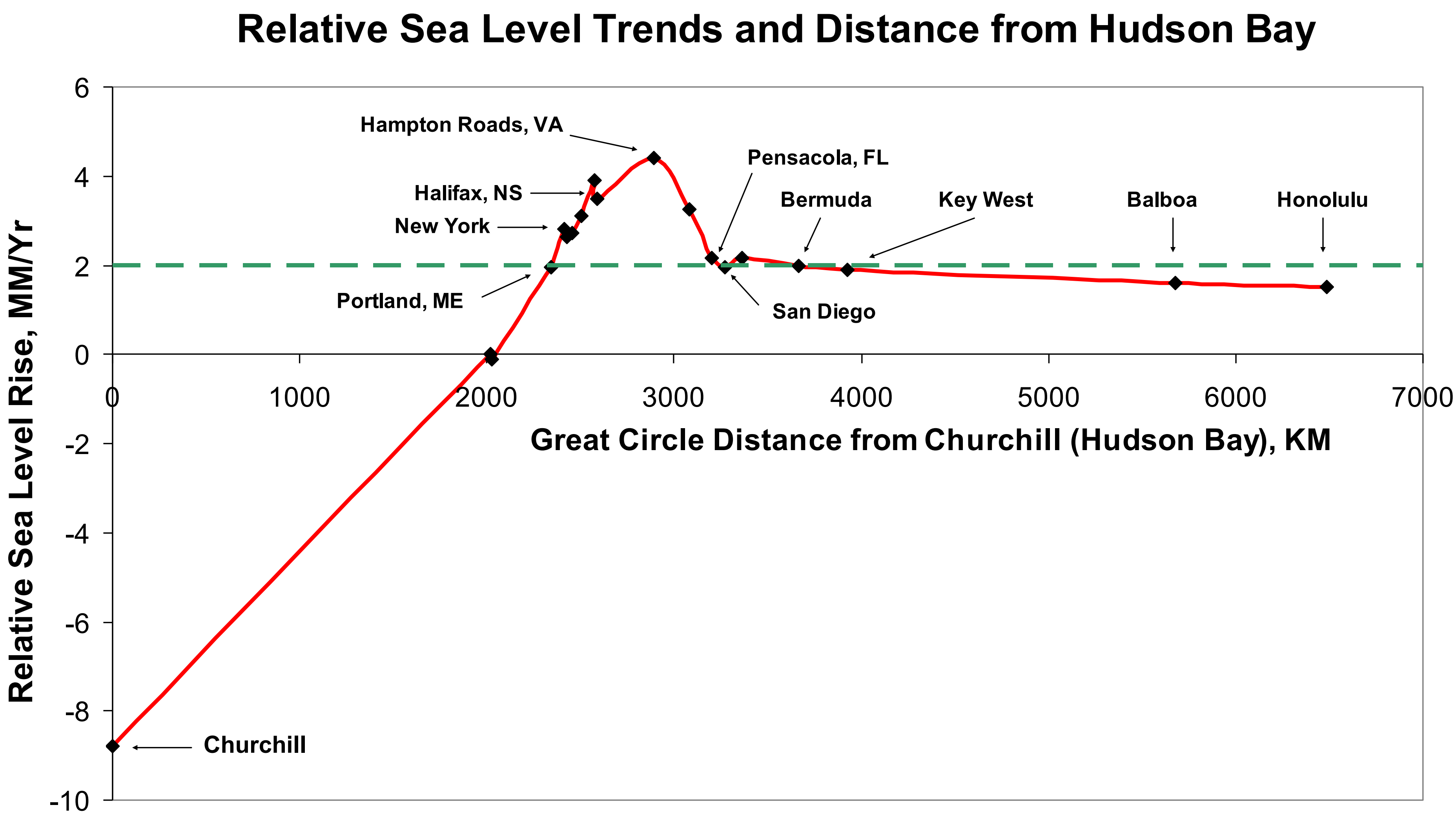

Miller L , and Douglas B C Phil. Trans. R. Soc. A 2006;364:805-820

RSL from tide gauges - Fennoscandia

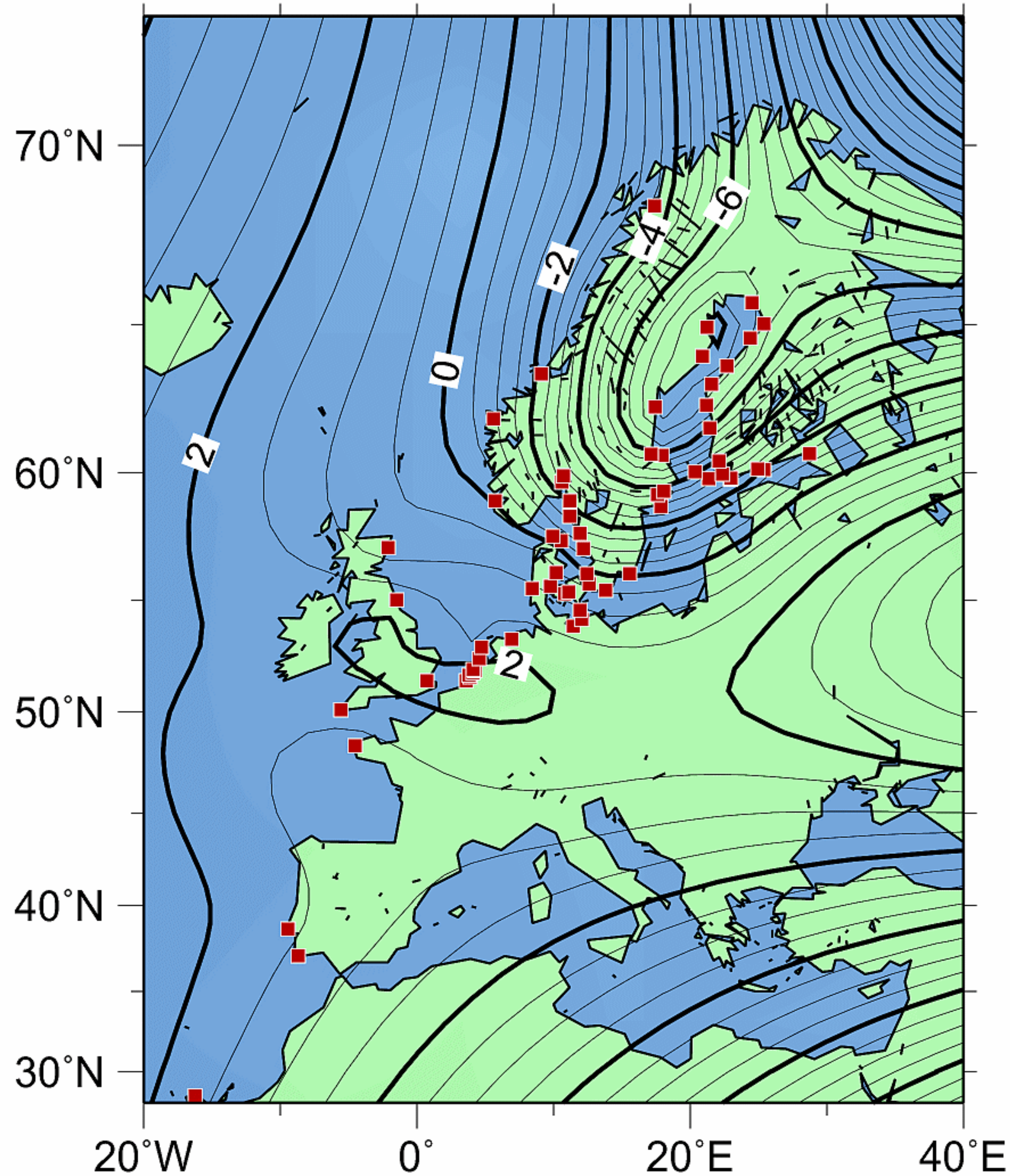

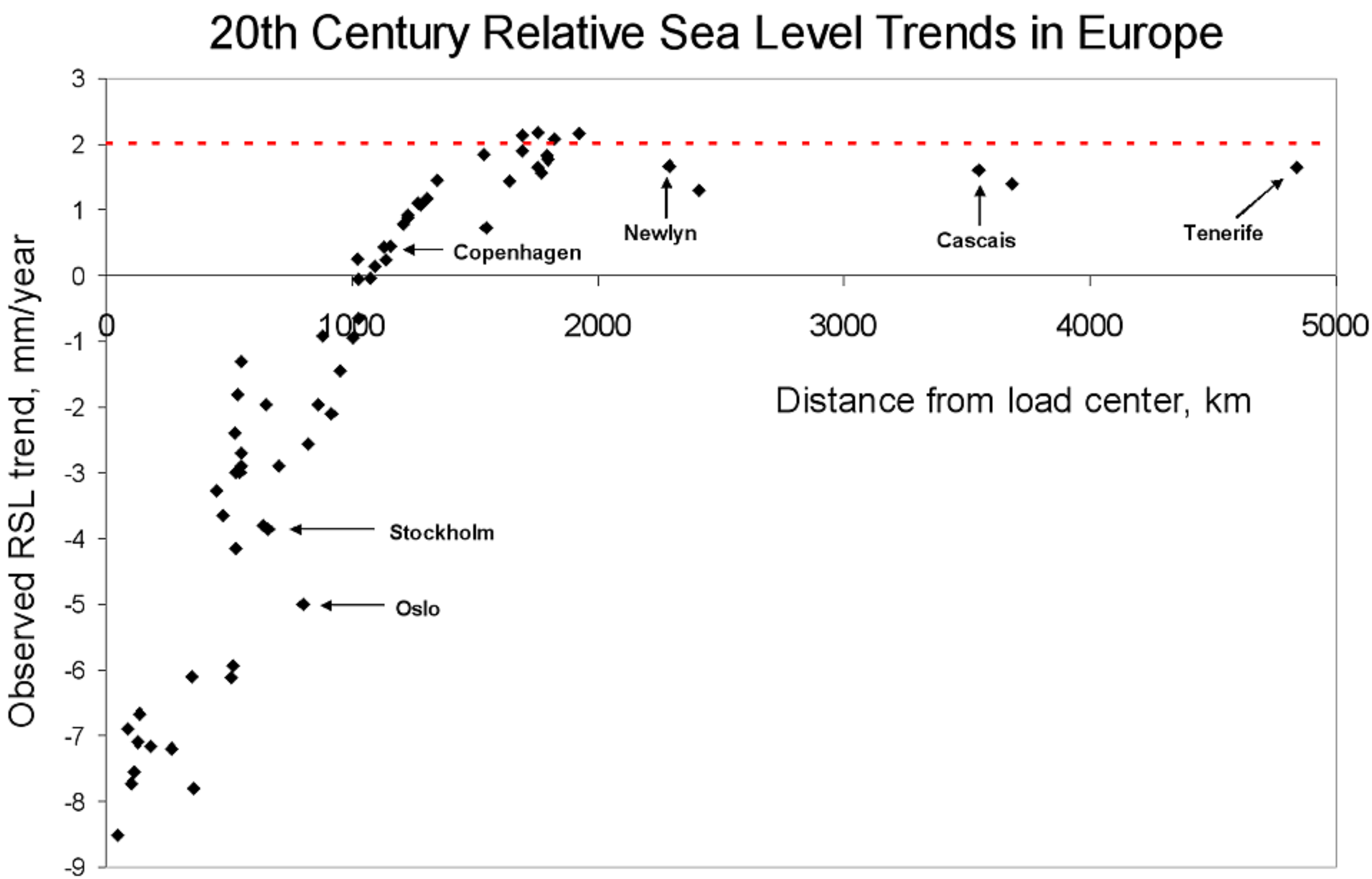

Miller L , and Douglas B C Phil. Trans. R. Soc. A 2006;364:805-820

Rebound at Greenland:
Present-day elastic rebound or past viscoelastic rebound?

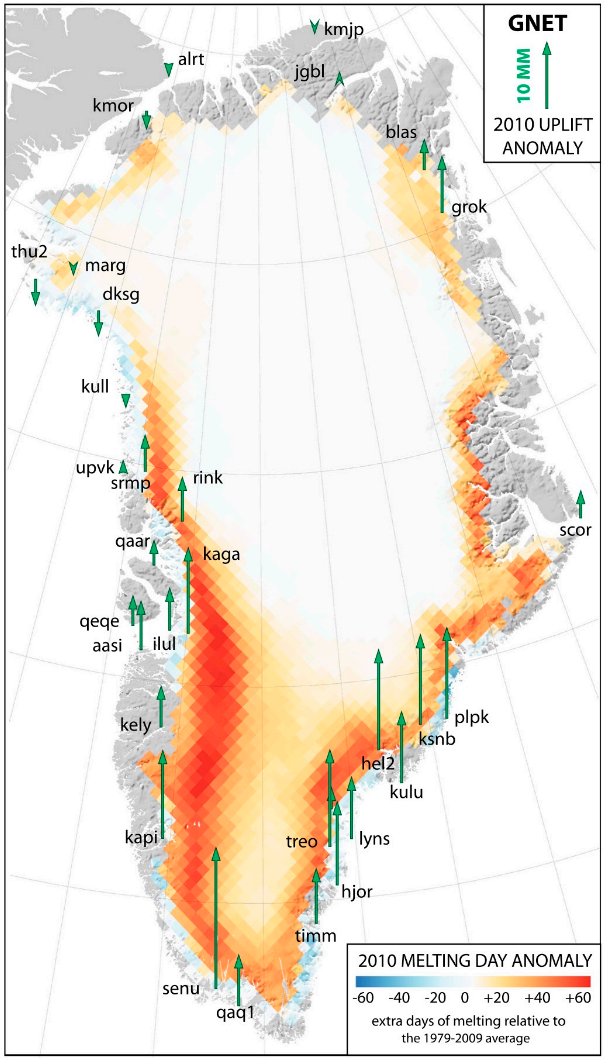

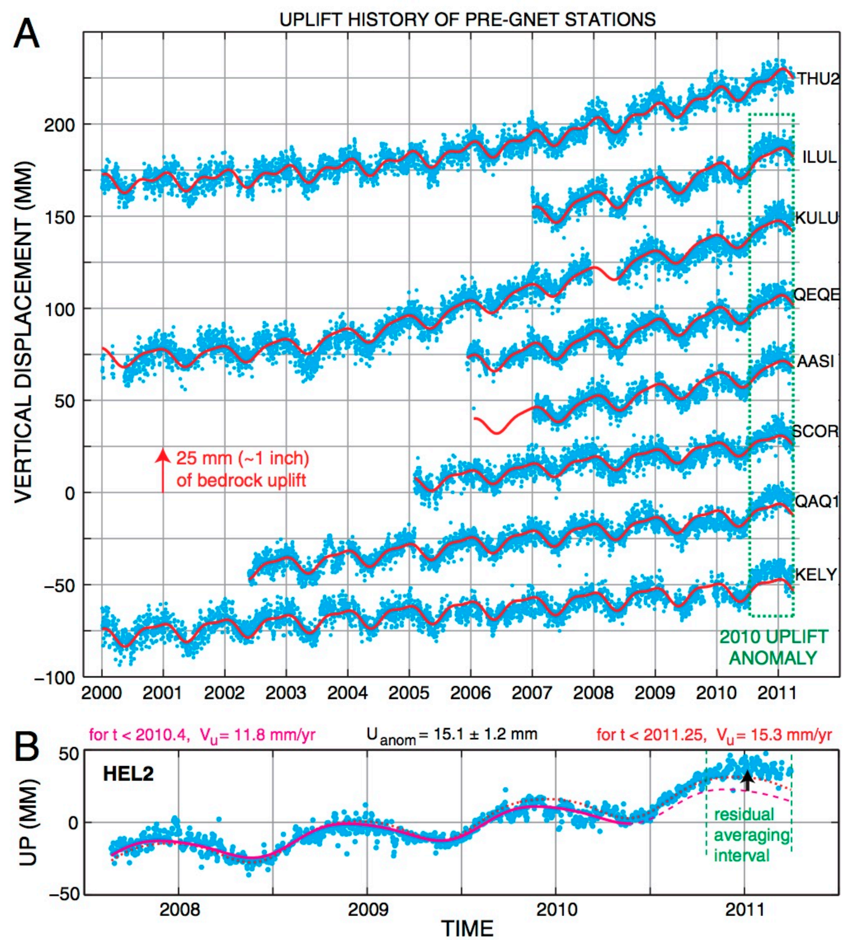

[Bevis et al., 2012]

vertical crustal motion from earthquakes

Great Sumatra Earthquake, 2004

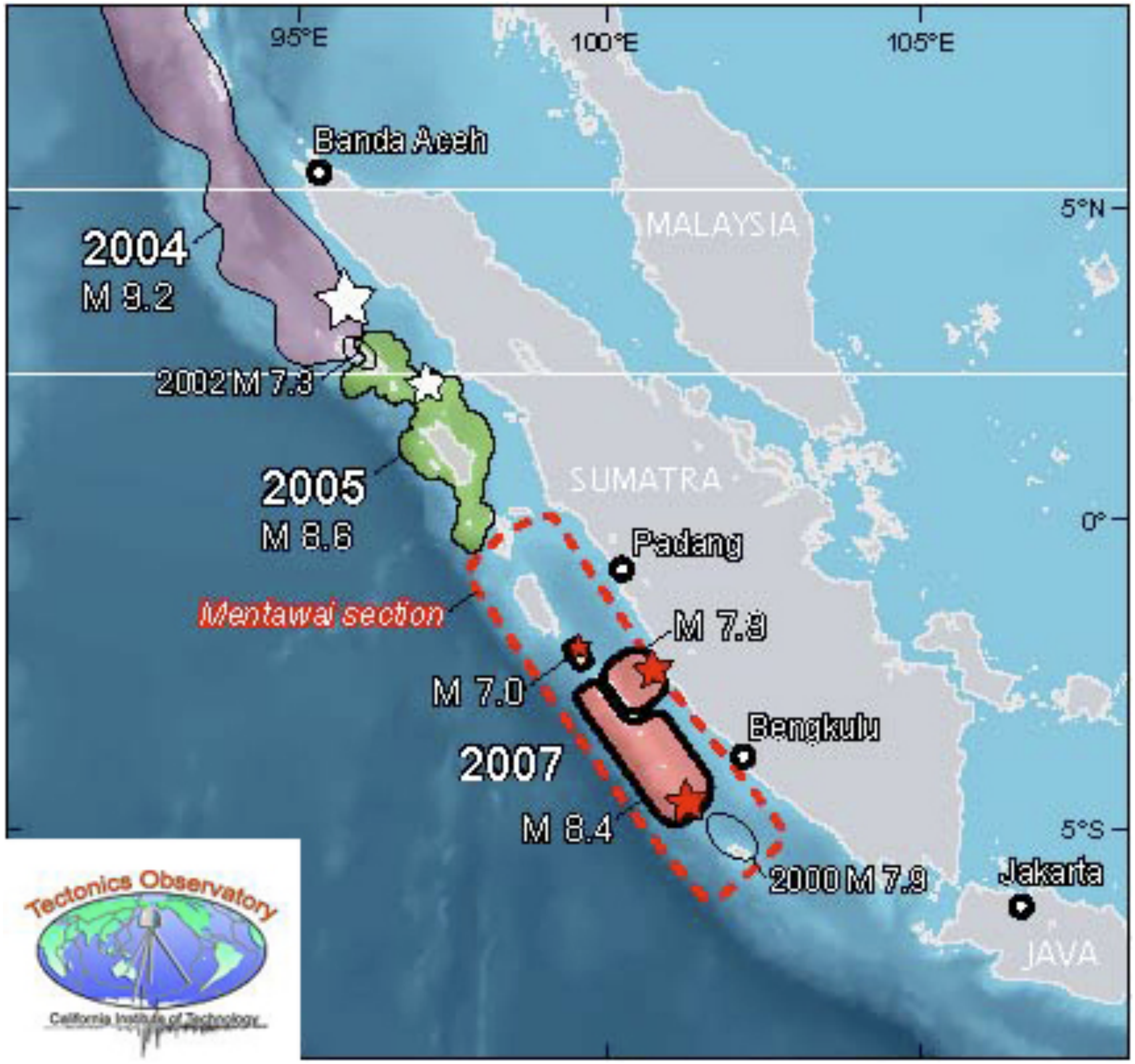

Great Sumatra Earthquake, 2004

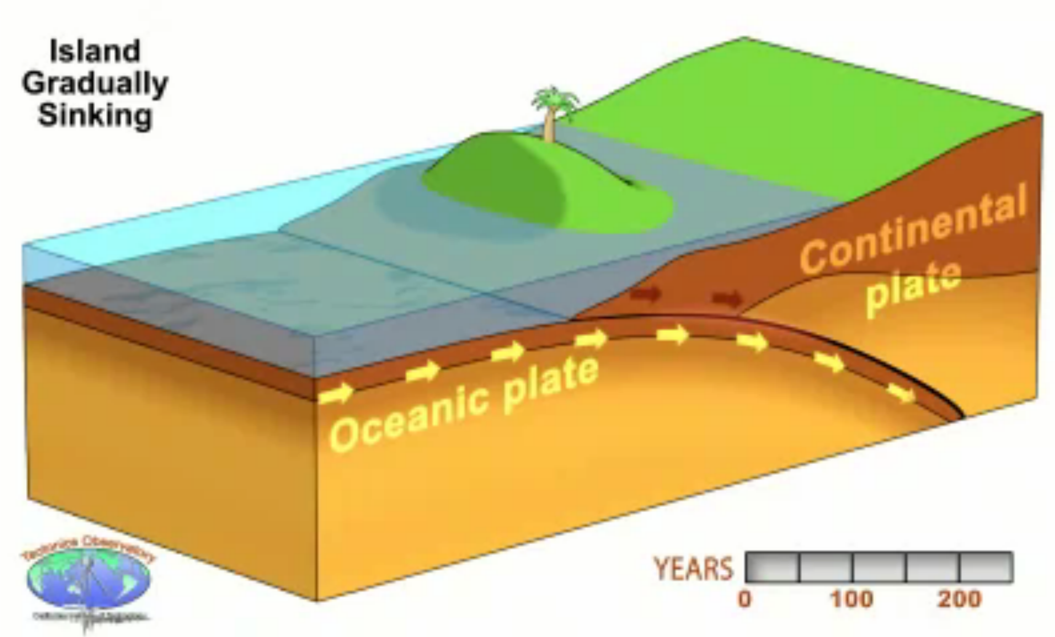

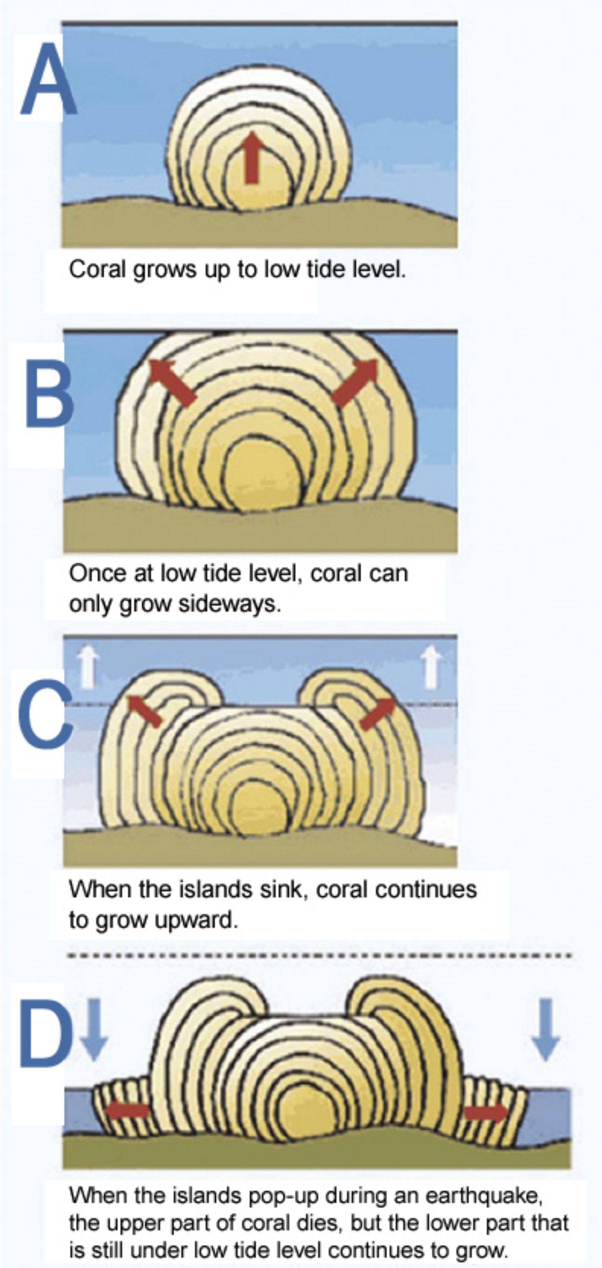

Sieh et al., Science, 2008

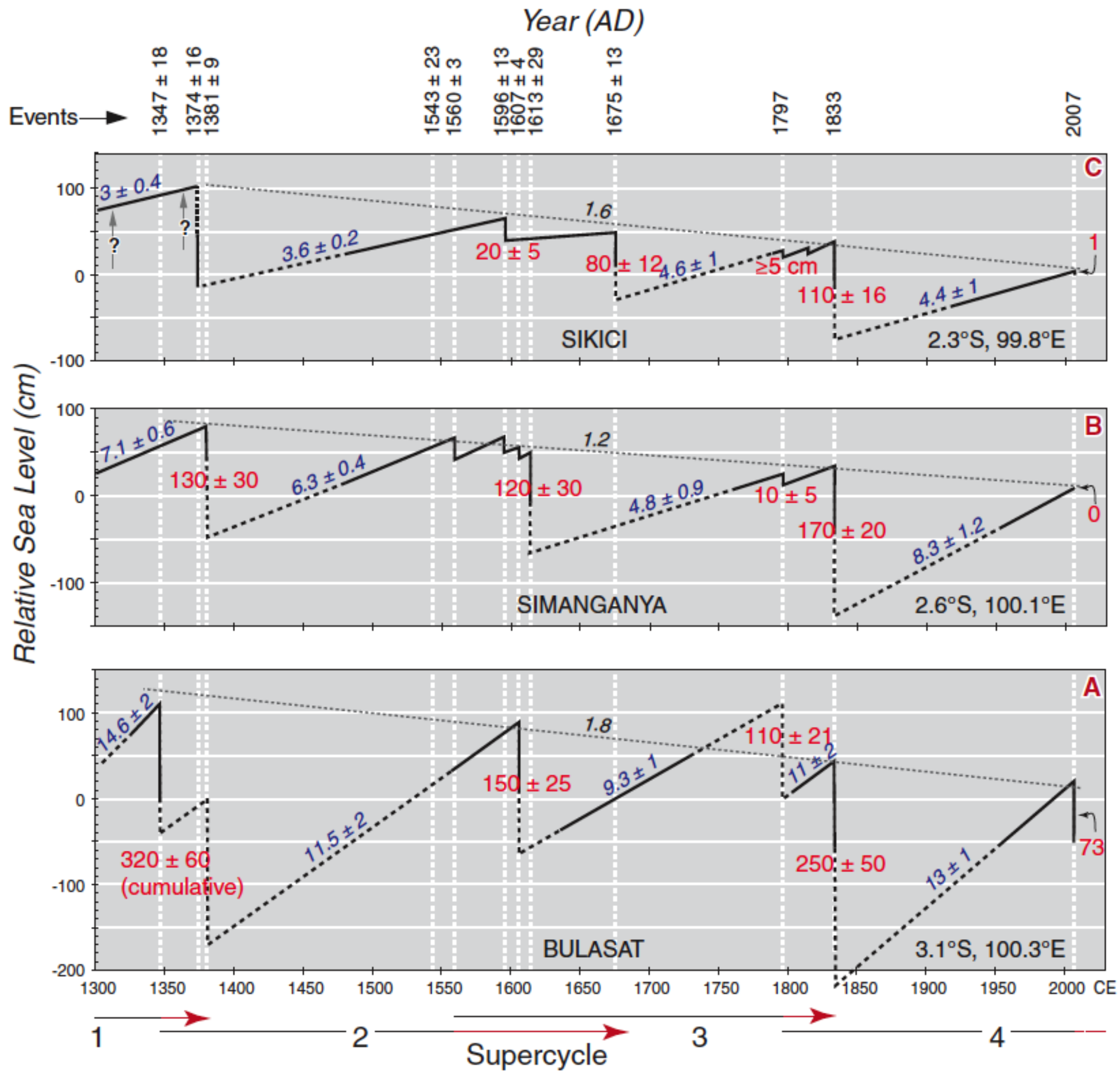

Fig. 2. Histories of interseismic submergence and coseismic emergence through seven centuries at sites (**A**) Bulasat, (**B**) Simanganya, and (**C**) Sikici. Data constrain solid parts of the curves well (fig. S4); dotted portions are inferred. Emergence values (in centimeters ± 2σ) are red. Interseismic submergence rates (in millimeters per year, ± 2σ) are blue. Millennial emergence rates are black. Vertical dashed white lines mark dates of emergences. Red arrows at bottom highlight the timing of the failure sequence for each supercycle.

vertical surface deformation from withdrawal of crustal fluids - water and oil

Annual groundwater recharge in LA Basin

(Watson et al., JGR 2001)

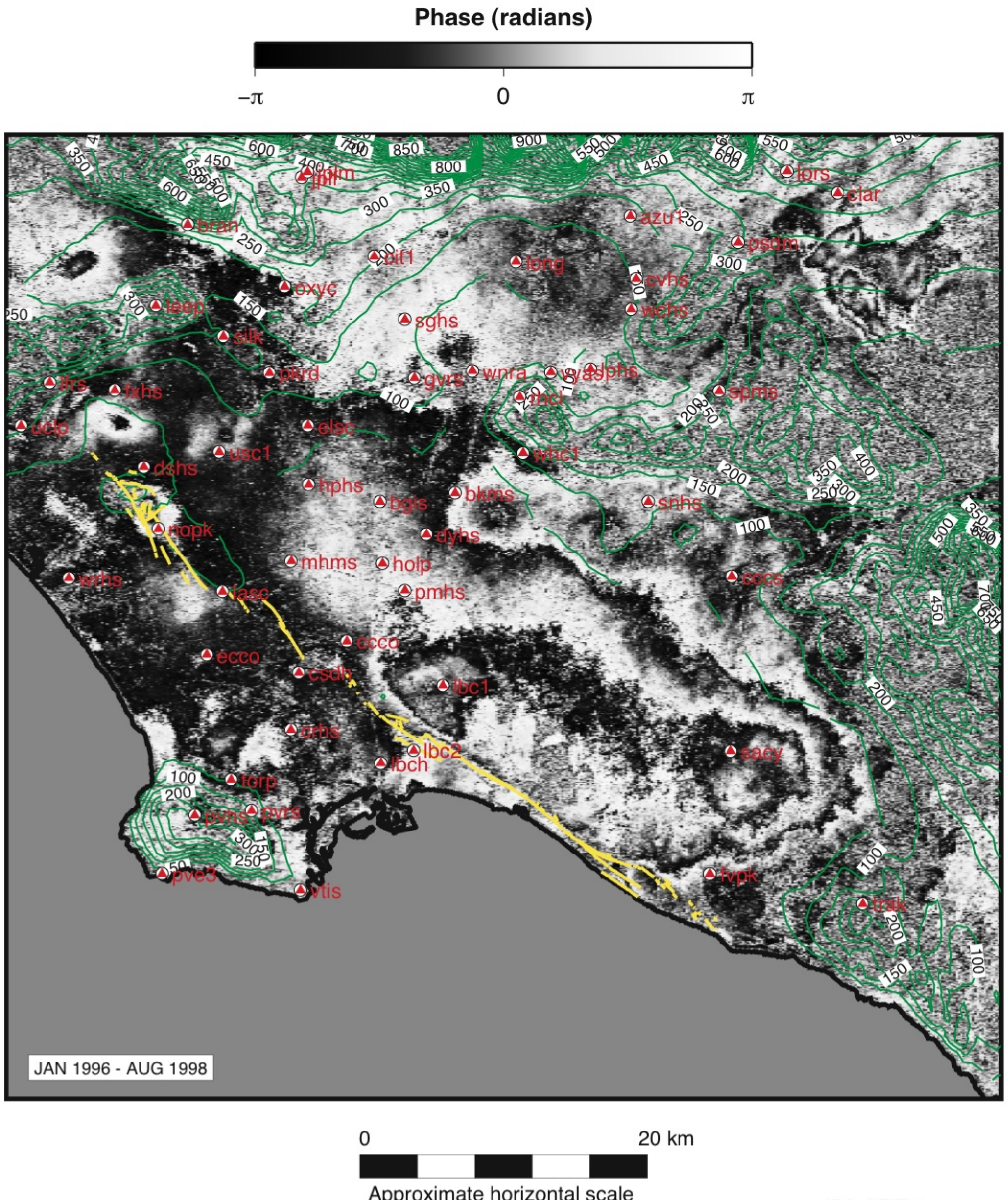

PLATE 1

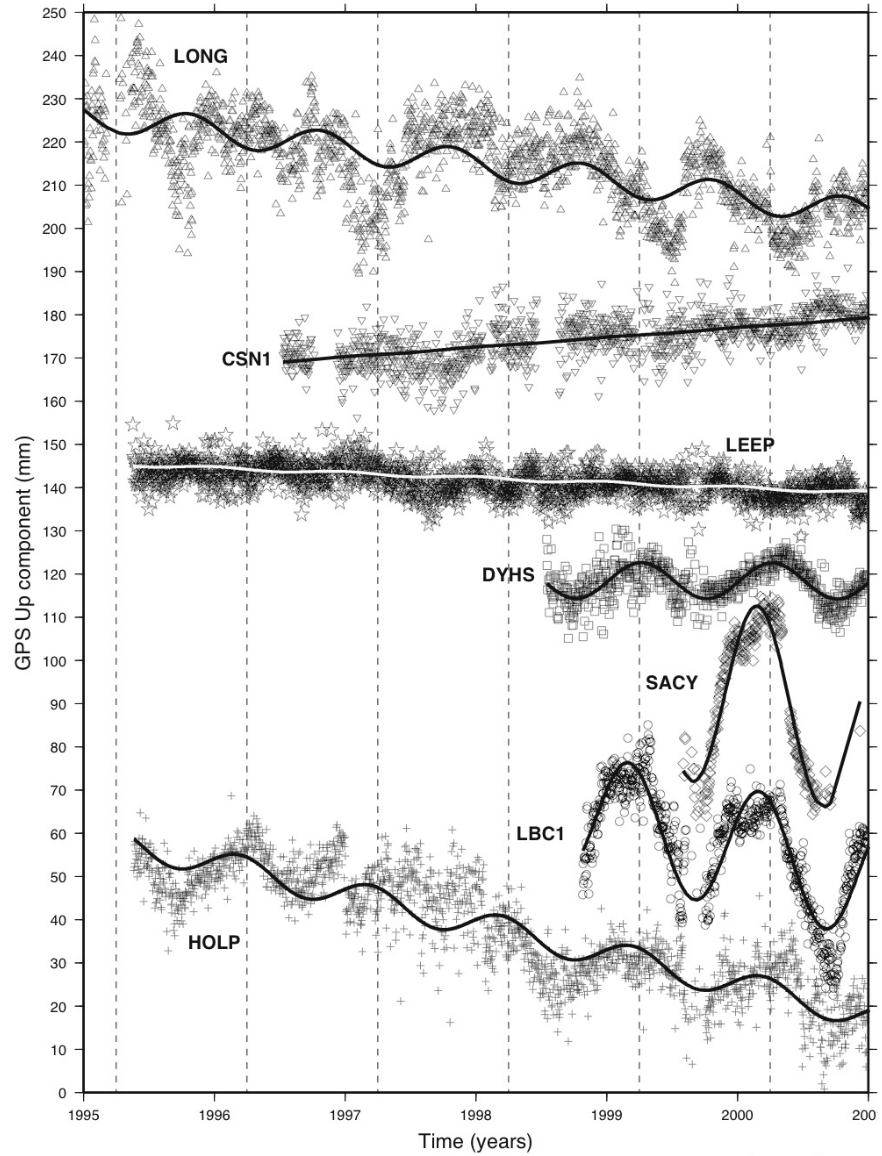

Figure 4

Groundwater in LA Basin

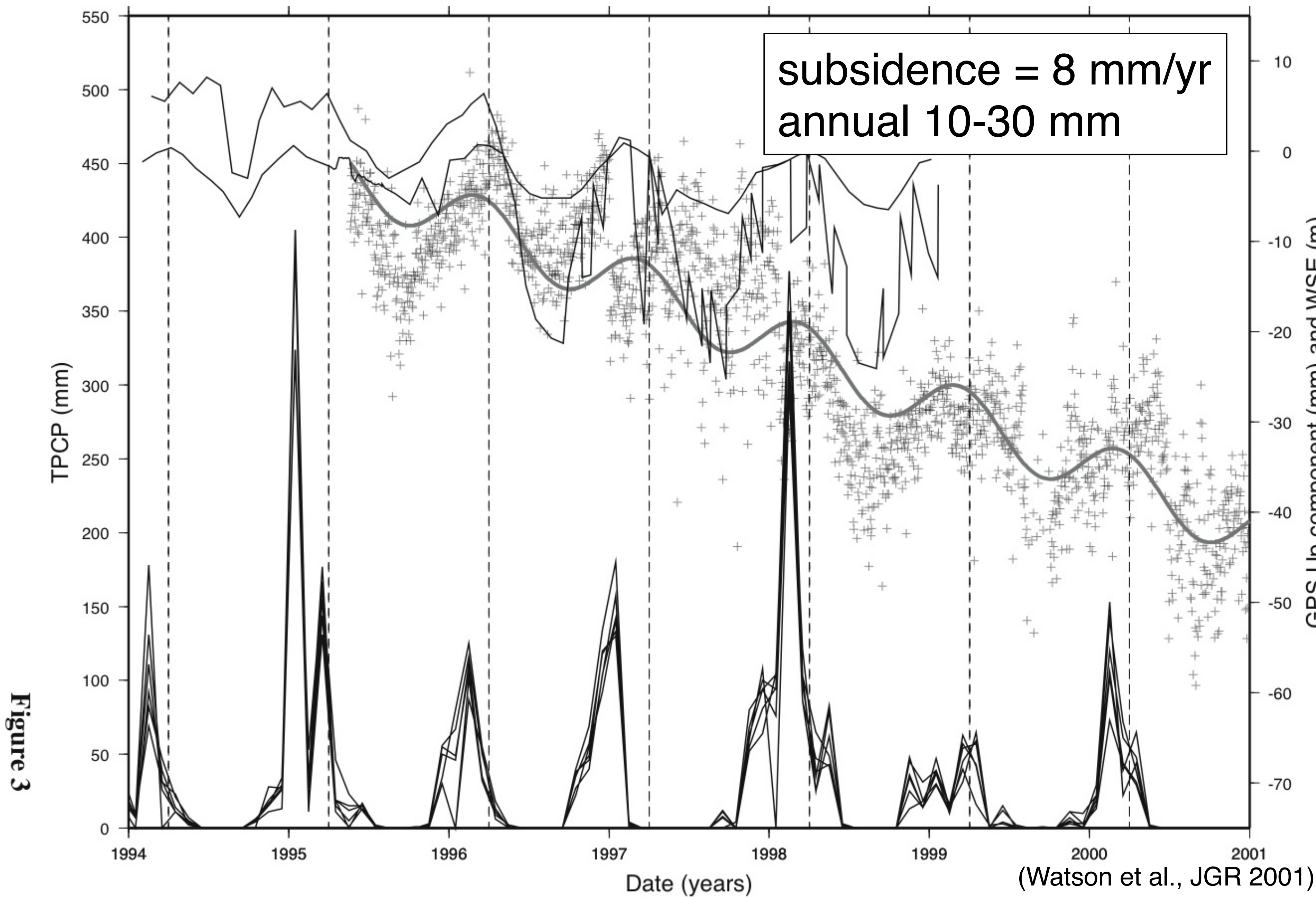

(Watson et al., JGR 2001)

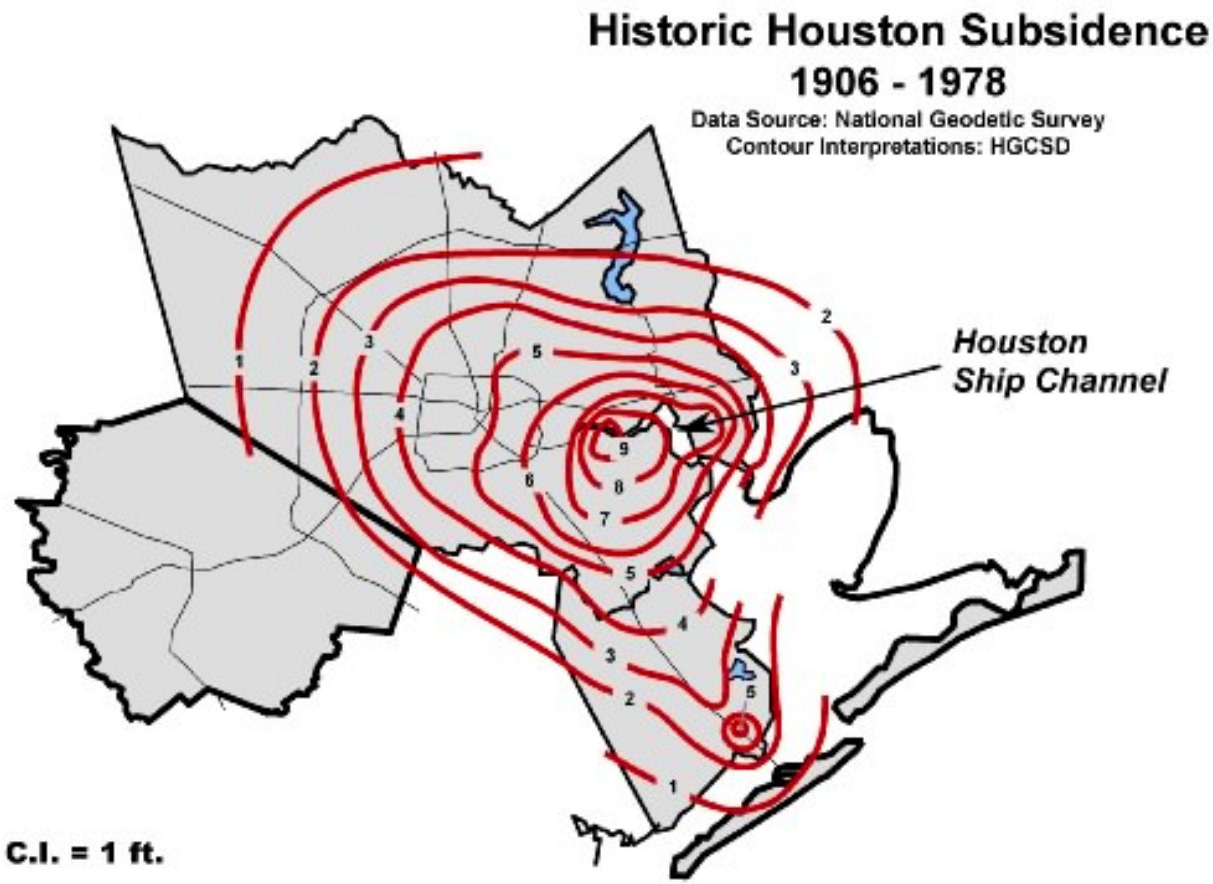

Figure 3. Subsidence occurring between 1906 and 1978 in the Houston-Galveston region, Texas. Map courtesy of Houston-Galveston Coastal Subsidence District

By 1979, the Houston Ship Channel area had subsided as much as 10 feet and over 3200 square miles of the Houston metropolitan area had sunk an average of one foot (Galloway et al, 1999). Most of Houston's subsidence is due to compaction of subsurface clays because of withdrawal of ground water from surrounding aquifer beds (Zilkoski et al, 2001).

maximum subsidence rate = 40 mm/yr

Berman, 2005

The first documented instance of land subsidence due to fluid withdrawal was from the Goose Creek oil field near the city of Houston. In 1917 oil was discovered on the margin of Galveston Bay near the mouth of the present-day Houston Ship Channel. After production of several million barrels of oil, bay waters began to inundate the oil field. (Figure 1). Pratt and Johnson (1926) recognized newly formed faults and fissures that resulted from fluid withdrawal (Figure 2).

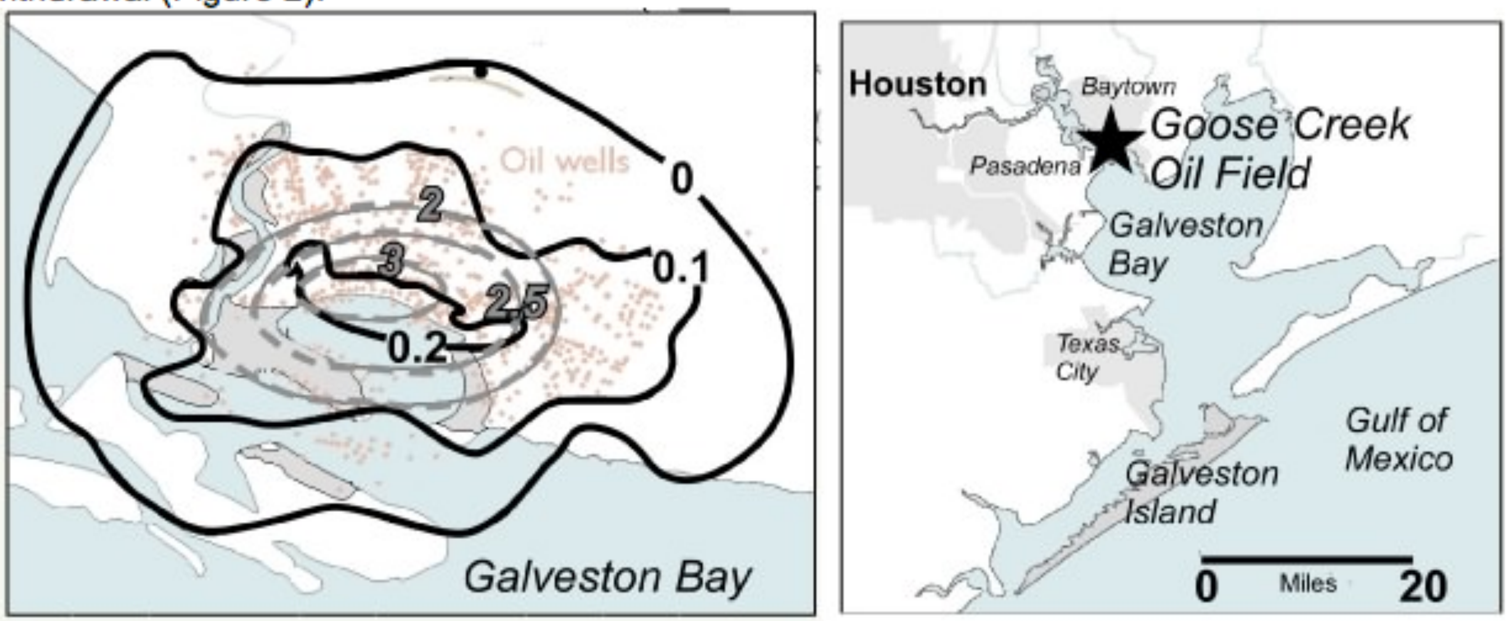

Figure 1. Measured subsidence between 1918 and 1926 around Goose Creek oilfield. Lines of equal subsidence (feet) for an 8-year period are shown in gray lines—for a 1-year period, in black lines. Modified from Galloway et al, 1999.

maximum subsidence rate = 100 mm/yr

Berman, 2005

Coastal Cities

Nelson 2009

The table below shows a list of cities throughout the world that have been experiencing subsidence problems. Note that most of these cities are coastal cities like London, Houston, and Venice, or are built on river flood plains and deltas, like New Orleans, Baton Rouge, and the San Joaquin Valley of central California. Mexico City is somewhat different in that it was built in a former lake.

City	Maximum Subsidence (m)	Area (km^2)	Cause
LongBeach/Los Angeles	9.00	50	Petroleum withdrawl
San Joaquin Valley, CA	8.80	13,500	Groundwater withdrawal
Mexico City	8.50	225	filled lake
Tokyo, Japan	4.50	3,000	coastal sediments
San Jose, CA	3.90	800	bay sediments
Osaka, Japan	3.00	500	coastal sediments
Houston, TX	2.70	12,100	coastal sediments
Shanghai, China	2.63	121	coastal sediments
Niigata, Japan	2.50	8,300	coastal sediments
Nagoya, Japan	2.37	1,300	coastal sediments
New Orleans, LA	2.00	175	river sediments
Taipei, China	1.90	130	coastal sediments
Bankok, Thailand	1.00	800	river sediments
Venice, Italy	0.22	150	coastal sediments
London, England	0.30	295	river sediments

Vertical Crustal Motions can dominate RSL

Global sea level rise ~3 mm/yr

Post Glacial Rebound 0-20 mm/yr

Earthquakes
- Sumatra subduction - 1000 mm
- California strike-slip - 200 mm

Interseismic
- Sumatra - 10 mm/yr
- California - 1.5 mm/yr

Groundwater
- LA - secular - 3 mm/yr (Long Beach)
- LA - annual - 10-30 mm/yr
- Houston - secular - 40 mm/yr
- New Orleans - secular - 8 mm/yr

OIL
- Houston (1920s) - 100 mm/yr